

# Competitive Energy and Electron-Transfer Quenching in Intramolecular Processes of Excited Polypyridine Ruthenium(II)/Osmium(II) Binuclear Complexes

M. Furue<sup>a</sup>, K. Maruyama<sup>a</sup>, Y. Kanematsu<sup>b</sup>, T. Kushida<sup>b</sup>, and M. Kamachi<sup>a</sup>

<sup>a</sup> Department of Macromolecular Science, Faculty of Science, Osaka University, Toyonaka, Osaka 560, Japan

<sup>b</sup> Department of Physics, Faculty of Science, Osaka University, Toyonaka, Osaka 560, Japan

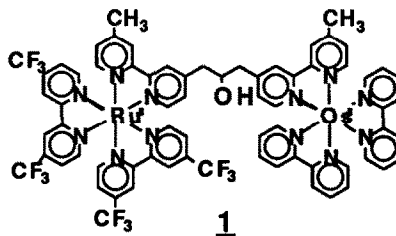
## ABSTRACT

In the excited state of the covalently bridged Ru(II)/Os(II) binuclear complex, [BTFMB<sub>2</sub>Ru(II)MebpyCH<sub>2</sub>CH(OH)CH<sub>2</sub>MebpyOs(II)(bpy)<sub>2</sub>] (BTFMB = 4,4'-bis-trifluoromethyl-2,2'-bipyridine), **1**, a nearly complete quenching of Ru(II) →  $\pi^*$  (BTFMB) MLCT emission was observed at room temperature. Lifetime measurements were performed to evaluate the quenching rate and the mechanism on a quantitative basis. In methanol at 298 K, the rate of reductive quenching of  $^*Ru(II)$  by Os(II) ( $k_{el}$ ) is  $5.3 \times 10^8 \text{ s}^{-1}$  and the rate of energy transfer from  $^*Ru(II)$  to Os(II) ( $k_{en}$ ) is  $7.8 \times 10^7 \text{ s}^{-1}$ . In n-butanol both processes are competitive. Values of  $k_{el}$  and  $k_{en}$  are  $1.8 \times 10^8 \text{ s}^{-1}$  and  $1.7 \times 10^8 \text{ s}^{-1}$ , respectively. It is shown that the relaxation dynamics of solvent plays an important role in the intramolecular electron-transfer process in protic media even when the observed rate is slow with respect to the solvent motion. The dipole-dipole interaction (Förster mechanism) is proposed for the energy-transfer mechanism.

## A. INTRODUCTION

The evaluation of the rate constant of the intramolecular step is crucial to understand the role of the various molecular parameters in determining reaction rates. The supramolecular systems allow the study of the effects of distance and driving force on electron and energy-transfer rates and afford a valuable opportunity for testing theoretical models [1,2].

The excited-state properties of poly-pyridine complexes of d<sup>6</sup> transition-metals such as Ru(II), Os(II), and Re(I) can be tuned by ligands and solvent environment [3]. Recently we have synthesized a new class of bipyridine ligands



containing a trifluoromethyl group as a substituent. 4,4'-Bistrifluoromethyl-2,2'-bipyridine (BTFMB) ligand has a lower lying  $\pi^*$  level which not only leads to significant changes in ground- and excited-state redox potentials but also exerts relatively large effects on absorption and emission spectral properties [4].

In this paper we report results showing that competitive energy and electron-transfer quenching of excited Ru(II) by Os(II) complex occurs intramolecularly in the title complex **1**. The kinetic study by the time-correlated single-photon counting method was performed to evaluate the quenching rate and the mechanism on the quantitative basis. The results have evidenced that the relaxation dynamics of solvent plays an important role in the intramolecular electron-transfer process and that the energy-transfer process can be interpreted in terms of the Förster mechanism.

## B. EXPERIMENTAL

**Materials.** BTFMB and **1** were synthesized by the same procedure as previously reported by us [4,5].

**Measurement.** Steady-state and time-resolved emission studies were carried out using procedures that have been previously described [5]. Electrochemical measurements were made in acetonitrile (MeCN) by using the same instrumentation and procedures as reported elsewhere [5].

## C. RESULTS AND DISCUSSION

In Fig. 1 are presented absorption spectra for **1** and its component complexes,  $[\text{Ru}(\text{BTFMB})_2\text{bpy}^{2+}]$ , **2**, and  $[\text{Os}(\text{dmb})_2\text{bpy}^{2+}]$ , **3** at the same substrate concentration. The spectrum of **1** was identical with the superimposed spectrum of equimolar concentration of its component complexes, **2** and **3**. Compared with  $\text{Ru}(\text{bpy})_3^{2+}$ , lower energy-shift from 450 to 475.5nm of metal-to-ligand charge-transfer (MLCT) band was observed for **2**, showing that BTFMB ligand has a lower lying  $\pi^*$  level.

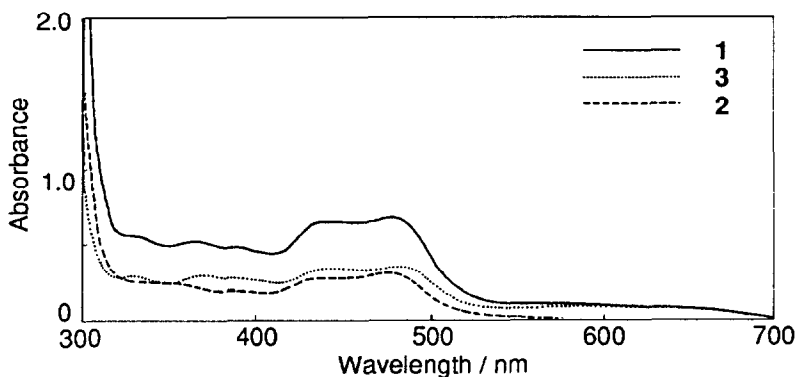


Fig. 1. Absorption spectra of **1**, **2**, and **3** in MeOH. [Substrate] =  $2.2 \times 10^{-5}$  M.

TABLE 1

Redox potentials for **1** and its model complexes. a)b)c)

| Complex               | $E_{1/2}$ / V vs. SCE |            |                             |                             |                 |                 |
|-----------------------|-----------------------|------------|-----------------------------|-----------------------------|-----------------|-----------------|
|                       | Ru(III/II)            | Os(III/II) | $(L^{0/-})_1$ <sup>d)</sup> | $(L^{0/-})_2$ <sup>d)</sup> | $(bpy^{0/-})_1$ | $(bpy^{0/-})_2$ |
| <b>1</b>              | +1.48 (70)            | +0.76 (80) | -0.94 (60)                  | -1.14 (70)                  | -1.33 (60)      | -1.51 (60)      |
| <b>2</b>              | +1.46 (80)            |            | -0.94 (60)                  | -1.14 (70)                  |                 | -1.87 (70)      |
| <b>3</b>              |                       | +0.73 (70) |                             |                             | -1.36 (70)      | -1.56 (75)      |
| <b>6<sup>e)</sup></b> | +1.19 (70)            |            |                             |                             | -1.36 (70)      | -1.56 (75)      |

a) Redox potentials [V vs SCE,  $E_{1/2} = (E_{pa} + E_{pc})/2$ ] were estimated from CV.Solvent : MeCN. Sweep rate : 100mV/sec. b) All complexes are PF<sub>6</sub> salts. c)Values in parenthesis are peak separation in mV. d) L = BTfMB. e) **6** =Ru(bpy)<sub>2</sub>(dmb)<sup>2+</sup>. bpy : 2,2'-bipyridine, dmb : 4,4'-dimethyl-2,2'-bipyridine

**1** shows two reversible oxidation waves at 1.46 V and 0.73 V vs. SCE for the Ru(III)/Ru(II) and Os(III)/Os(II) couples, and four reversible waves at -0.94, -1.14, -1.33, and -1.51 V vs. SCE for the ligand-based reduction for Ru and Os components. These values correspond to those of **2** and **3**, respectively. (Table 1) The sequence of reduction steps best interpreted as the stepwise reduction of each ligand  $\pi^*$  system. The strong  $\sigma$ -attracting CF<sub>3</sub> substituent is responsible for the shift of 0.5 V in 1st reduction of **2** vs. Ru(bpy)<sub>2</sub>dmb<sup>2+</sup>.

Room-temperature luminescence spectra of **1** (excitation wavelength : 455 nm) was recorded in argon-gas bubbled solutions and compared with those of **3** and [(bpy)<sub>2</sub>Ru(II)MebpyCH<sub>2</sub>CH(OH)-CH<sub>2</sub>MebpyOs(II)(bpy)<sub>2</sub>], **5** [6] at the same substrate concentration. As an illustration, the luminescence spectra of **1**, **3**, and **5** in n-BuOH are shown in Fig. 2. The efficient quenching of emission at 630 nm from the ruthenium complex was observed in **1** and **5**. More than 98% of the potential luminescence of their ruthenium component (as measured for **2**) was quenched in **1** and **5**. In the case of **5**, the enhancement of emission intensity at 750 nm from the osmium component was almost double in comparison with that of **3**. This indicates that the intramolecular energy-transfer process in **5** has a unitary efficiency [5,6]. On the other hand, the sensitization of the osmium component in **1** is in about 50% efficiency.

As for the quenching mechanism, energy transfer from <sup>\*</sup>Ru(II) to Os(II) and reductive electron transfer from Os(II) to <sup>\*</sup>Ru(II) are conceivable in the excited state of **1**. In acetonitrile, the first ligand-based reduction potential of BTfMB<sup>0/-</sup>

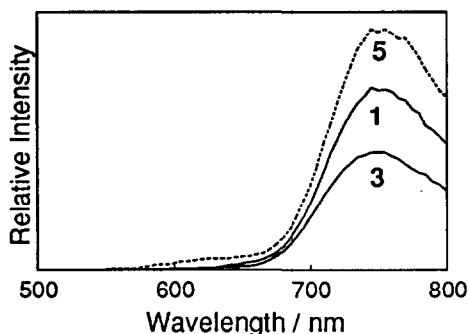


Fig. 2. Emission spectra of **1**, **3**, and **5** in 1-BuOH. [Substrate] =  $1.5 \times 10^{-5}$  M. Excitation at 455 nm.

couple and the first oxidation potential of the  $\text{Os}^{3+/2+}$  couple of **1** are -0.94 V and 0.76 V vs SCE, respectively. The excited-state energy of **2** was estimated to be 2.0 eV [7,8]. The value of 1.78 eV is reported for **3** [9]. The photophysical behavior can be described in terms of an energy level diagram that is simply made by superimposing the low-lying excited states of the ruthenium and osmium units on the redox potentials in the ground state. As seen in Ru(bpy)-Os complex **5**, energy-transfer is also favorable by 0.22 eV in **1** which corresponds nearly to the observed difference in the emission maxima of **2** ( $E_{\text{em}} = 1.54 \times 10^4 \text{ cm}^{-1}$ ) and **3** ( $E_{\text{em}} = 1.33 \times 10^4 \text{ cm}^{-1}$ ). The reductive quenching of the excited Ru-complex is exergonic ( $\Delta G = -0.3 \text{ V}$ ) based on a reduction potential (1.06 V) for the  $\text{Ru}^{2+}/+$  couple

with the oxidation potential (0.76 V) for the  $\text{Os}^{3+/2+}$  couple. This is a remarkable feature of **1**, while the electron-transfer quenching process is endergonic in **5**. The thermodynamical aspect allows us to conclude that both energy transfer and electron transfer constitute the quenching mechanism in the excited state of **1**.

The measurement of luminescence lifetime was performed to evaluate the quenching on a quantitative basis by a time-correlated single-photon counting method. The decay of  $\text{Ru}^{\text{II}} \rightarrow \pi^*(\text{bpy})$  MLCT emission at 630 nm and rise and decay of  $\text{Os}^{\text{II}} \rightarrow \pi^*(\text{bpy})$  MLCT emission at 800 nm were measured in various solvents (excitation wavelength at 457.9 nm and instrumental width of 300 ps). Fig. 3 shows luminescence profiles of **1** in MeOH at 273K, with which a computer-calculated fit is superimposed. The luminescence profile can be fit well by a convolution of a biexponential model  $I_{\text{v}}(t) = A_1 \exp(-t/\tau_1) + A_2 \exp(-t/\tau_2)$  and the experimental instrument response function. Typical sets of parameter with amplitudes represented as percentages are presented in figures. At 630 nm the best fit was obtained with  $\tau_1 = 2.3 \text{ ns}$  (98.5%) and  $\tau_2 = 320 \text{ ns}$  (1.5%) (Fig. 3a). A minor, long-lived component can be attributed to a mononuclear ruthenium complex. The fast exponential decay (2.3 ns) is attributed to the deactivation of the ruthenium-excited state by the intramolecular quenching process. In Fig. 3b, the double exponential analysis for the rise and decay of the excited osmium complex at 800 nm gave  $\tau_1 = 2.3 \text{ ns}$  and  $\tau_2 = 40.5 \text{ ns}$ . The ratio of the preexponential factor of the double exponential function, namely  $A_2/A_1$

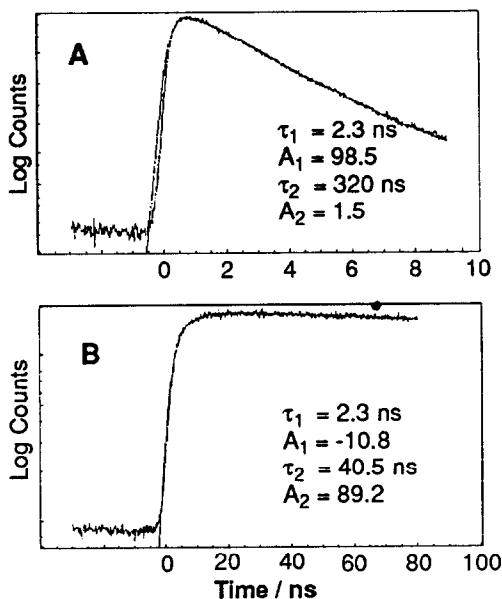
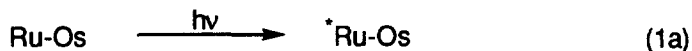


Fig. 3. Emission decay for **1** in MeOH at 273 K. Monitored at 630 (A) and 800 (B) nm. Excitation at 457.9 nm. A computer calculated fit is superimposed.

was -8.3. If the energy-transfer process has a unitary efficiency in this system,  $A_2/A_1$  should be close to -2.2. The deviation of  $A_2/A_1$  from -2.2 indicates the existence of additional intramolecular quenching-process besides the energy-transfer process (*vide infra*).

Kinetics of intramolecular processes in **1** was evaluated by the following scheme. The excitation at 457.9 nm of **1**, denoted by Ru-Os, affords two excited states, namely  $^*\text{Ru-Os}$  and  $\text{Ru-Os}^*$  (eq 1a and 1b). In addition to the normal deactivation process (eq 1c and 1f), the additional quenching of  $^*\text{Ru-Os}$  by an intramolecular electron-transfer process (eq 1d) and the buildup of  $\text{Ru-Os}^*$  by the intramolecular energy-transfer process (eq 1e) are taken into account:



and



The relevant rate equations are

$$d[^*\text{Ru-Os}]/dt = -(k_1 + k_{el} + k_{en})[^*\text{Ru-Os}] \quad (2a)$$

and

$$d[\text{Ru-Os}^*]/dt = k_{en}[^*\text{Ru-Os}] - k_2[\text{Ru-Os}^*] \quad (2b).$$

Equation (2b) yields

$$[\text{Ru-Os}^*] = A_1 \exp[-(1/\tau_1)t] + A_2 \exp[-(1/\tau_2)t], \quad (3)$$

where  $A_1 = k_{en}[^*\text{Ru-Os}]_0 / (1/\tau_2 - 1/\tau_1)$ ,  $A_2 = [\text{Ru-Os}^*]_0 - A_1$ ,  $1/\tau_1 = k_1 + k_{el} + k_{en}$ ,  $1/\tau_2 = k_2$ , and  $[^*\text{Ru-Os}]_0$  and  $[\text{Ru-Os}^*]_0$  denote the initial concentration of  $^*\text{Ru-Os}$  and  $\text{Ru-Os}^*$ , respectively.  $\tau_1$  can be obtained from the decay time at 630 nm and the rise time at 800 nm.  $\tau_2$  can be also obtained from the decay time at 800 nm. The values of  $k_2$  calculated from  $\tau_2$  are in the range of  $(2-5) \times 10^7 \text{ s}^{-1}$ . The value of  $k_1$   $\{(3-4) \times 10^6 \text{ s}^{-1}\}$  is based on the lifetime of its component complex, **2** at room temperature.

Molar absorption coefficients of its component complexes at 457.9 nm in MeOH are  $1.02 \times 10^4$  and  $1.22 \times 10^4 \text{ M}^{-1}\text{cm}^{-1}$  for **2** and **3**, respectively. The value of  $[^*\text{Ru-Os}]_0 / [\text{Ru-Os}^*]_0 (= 1.2)$  was used for all solvents in this paper. The ratio of the preexponential factors of eq 3 is given by  $A_2/A_1 = 1.2 \times (k_2 - k_1 - k_{el})/k_{en} \sim 2.2$ . (4)

The rate constants  $k_{el}$  and  $k_{en}$  can be calculated from the observed set of values of  $A_2/A_1$ ,  $\tau_1$ , and  $\tau_2$ . The values of  $k_{el}$  and  $k_{en}$  in various solvents at room

TABLE 2

Rate Constants of Intramolecular Electron and Energy-Transfer at Room Temperature and Kinetic Parameters for Electron-Transfer.

|                                   | H <sub>2</sub> O        | MeOH                    | EtOH                   | 1-PrOH | 1-BuOH |
|-----------------------------------|-------------------------|-------------------------|------------------------|--------|--------|
| $k_{el}$ , $10^8 \text{ s}^{-1}$  | 12.9                    | 5.3                     | 3.8                    | 2.7    | 1.8    |
| $E_a$ , Kcal/mol                  |                         | 2.1                     | 2.2                    |        | 1.6    |
| $A$ , $10^{10} \text{ s}^{-1}$    |                         | 1.6                     | 1.6                    |        | 0.3    |
| $\tau_L$ , $10^{-12} \text{ s}^b$ | 0.20                    | 3.3                     | 9.8                    | 42     | 80     |
| $k_{en}$ , $10^8 \text{ s}^{-1}$  | 0.79(4.5) <sup>a)</sup> | 0.78(3.7) <sup>a)</sup> | 1.5(3.3) <sup>a)</sup> | 1.2    | 1.7    |

a : Values in parentheses indicate  $k_{en}$  for Ru(bpy)-Os complex, **5**.

b : Longitudinal solvent relaxation time [10].

temperature are shown in Table 2. The rate constant of electron-transfer is markedly solvent dependent.

The temperature dependence of the rate was examined in the range of 293-243 K in several solvents. From a plot of  $\ln k_{el}$  versus  $T^{-1}$ , the values of activation energy ( $E_a$ ) and the frequency factor ( $A$ ) were calculated and shown in Table 2.

In semiclassical theory [11], the rate constant ( $k_{el}$ ) for a (first order) electron-transfer reaction can be given by

$$k_{el} = \kappa_{el} \nu_n \exp \left[ \frac{-(\Delta G^\circ + \lambda)^2}{4\lambda RT} \right] \quad (5)$$

where  $\kappa_{el}$  is the electronic transmission coefficient between the donor and acceptor,  $\nu_n$  is the frequency factor of the nuclear motion that takes the system over the barrier,  $\Delta G^\circ$  is the energy gap for the reaction,  $\lambda$  is a reorganizational parameter,  $R$  is the gas constant, and  $T$  is the absolute temperature.

The activation energy  $E_a$  corresponds to the height of the nuclear barrier, namely  $(\Delta G^\circ + \lambda)^2/4\lambda$ . In the present protic media,  $E_a$  did not change much, whereby the solvent is not considered to affect the reaction rates via its influence on the net activation barrier to electron transfer. (Table 2) In the nonadiabatic limit the frequency factor  $A$  is given by  $A = \kappa_{el} \nu_n = (2\pi\hbar)(H_{AB})^2(4\pi\lambda RT)^{-1/2}$ , with  $H_{AB}$  being the electronic coupling matrix element. In the adiabatic limit the frequency factor is proportional to the inverse longitudinal dielectric relaxation time  $\tau_L^{-1}$ , i.e.  $A = \nu_n = (\tau_L)^{-1}(\lambda/16\pi RT)^{1/2}$ , where  $\tau_L = (\epsilon_\infty/\epsilon_s)\tau_D$  with  $\epsilon_\infty$  and  $\epsilon_s$  being the optical and the static dielectric constants, respectively, while  $\tau_D$  is the Debye dielectric relaxation time [12]. An explicit decrease of  $A$  from ethanol to BuOH may suggest the adiabatic character in the intramolecular electron-transfer in alcohols. There

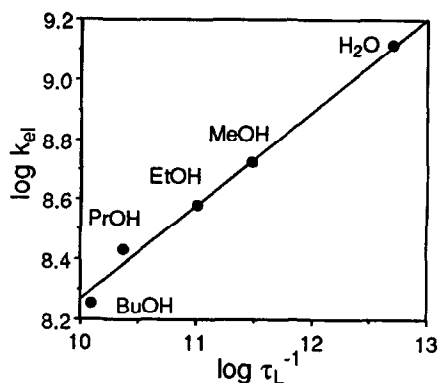


Fig. 4. Logarithmic plot of  $k_{el}$  vs. the inverse longitudinal dielectric relaxation time  $\tau_L^{-1}$  of solvents

have been several examples of the adiabatic behavior in bichromophoric systems where donor/acceptor sites are separated by several  $\sigma$ -bonds [13-15]. In this respect we examined the relationship between the rate constants of intramolecular electron transfer and the relaxation time of the solvent. Fig. 4 shows a logarithmic plot of  $k_{el}$  at room temperature versus inverse of longitudinal relaxation time,  $\tau_L^{-1}$ .  $k_{el}$  and  $\tau_L$  values are given in Table 2. A nearly linear dependence of  $k_{el}$  on  $\tau_L^{-1}$  is obvious. This finding suggests that the intramolecular electron-transfer process in the excited **1** is weakly adiabatic and is dominated by the relaxation dynamics of solvent even when the observed rate is slow with respect to the solvent motion.

The mechanisms available for the transfer of electronic energy are based on remote dipole-dipole or dipole-multipole electronic interactions (the Förster mechanism) [16] and on a collisional mechanism that involves electronic exchange (the Dexter mechanism) [17]. A quantitative treatment of the Förster mechanism leads to the following expression for  $k_{en}$ : [16]

$$k_{en} = \frac{9000 \ln 10 \kappa^2 \Phi_D}{128 \pi^5 n^4 N \tau_D r^6} \int_0^\infty F_D(\nu) \epsilon_A(\nu) \frac{d\nu}{\nu^4} \quad (6)$$

Here,  $\nu$  is the wave number,  $F_D(\nu)$  is the spectral distribution of the donor emission in quanta normalized to unity,  $\epsilon_A(\nu)$  is the molar extinction coefficient for the acceptor absorption,  $n$  is the refractive index of the solvent,  $\kappa$  is an orientation factor which equals  $(2/3)^{1/2}$  for a random distribution of donor and acceptor molecules,  $\Phi_D$  is the quantum yield of donor emission,  $\tau_D$  is the actual donor emission lifetime,  $N$  is Avogadro's number, and  $r$  is the distance between the donor and acceptor molecules. The overlap integral was calculated from numerical integration over the emission of **2** and the absorption of **3** in various solvents. The values are in the range of  $(2.4-2.9) \times 10^{-14} \text{ mol}^{-1} \text{ cm}^6$ . Assuming  $\kappa^2 = 2/3$  and  $r = 13 \text{ \AA}$  for **1**, the calculated  $k_{en}$  values were listed in Table 4. The calculated  $k_{en}$  values were reasonably close to the observed values.

Table 4.  
Rate Constants of Energy Transfer Calculated from Förster Equation.

| Solvent          | n     | $\Phi_D$ | $\tau_D$ / ns | Overlap Int.          | $k_{en}(\text{calc}) / \text{s}^{-1}$ | $k_{en}(\text{obs}) / \text{s}^{-1}$ |
|------------------|-------|----------|---------------|-----------------------|---------------------------------------|--------------------------------------|
|                  |       |          |               |                       |                                       | 1                                    |
| H <sub>2</sub> O | 1.333 | 0.018    | 250           | $2.8 \times 10^{-14}$ | $7.8 \times 10^7$                     | $7.9 \times 10^7$                    |
| MeOH             | 1.327 | 0.029    | 320           | $2.8 \times 10^{-14}$ | $1.0 \times 10^8$                     | $7.8 \times 10^7$                    |
| EtOH             | 1.359 | 0.033    | 360           | $2.9 \times 10^{-14}$ | $9.6 \times 10^7$                     | $1.5 \times 10^8$                    |
| 1-PrOH           | 1.384 | 0.036    | 340           | $2.9 \times 10^{-14}$ | $1.0 \times 10^8$                     | $1.2 \times 10^8$                    |
| 1-BuOH           | 1.397 | 0.032    | 345           | $2.4 \times 10^{-14}$ | $7.2 \times 10^7$                     | $1.7 \times 10^8$                    |

It is known that the excited electron in MLCT excited state of  $\text{Ru}(\text{bpy})_3^{2+}$  is fully localized on one of three equivalent ligands, at least for a time long enough

for this ligand and its neighboring solvent to adjust to the geometry of fully charged  $\text{bpy}^-$ . Picosecond transient Raman studies on mixed-ligand derivatives of Ru(II) complexes have also shown that the optical electron is localized on the most easily reduced ligand [18]. In **1**, MLCT excitation takes place exclusively from ruthenium to bis(trifluoromethyl)bpy ligand (BTfMB). In this case the through-space interaction can be more feasible than the through-bond interaction. Therefore it is reasonable to conclude that the dipole-dipole interaction, namely the Förster mechanism, is the main pathway for intramolecular energy transfer in the excited **1**.

Our results show that the introduction of BTfMB ligand onto the Ru(II)/Os(II) binuclear system results in competition of intramolecular energy and electron-transfer quenching and that solvent can play the important role in governing the rate of intramolecular electron transfer.

#### D. ACKNOWLEDGMENT

We are indebted to Dr. Koichi Nozaki (Chemistry Department, College of General Education, Osaka University) for interesting and helpful discussion.

#### E. REFERENCES

- (1) M.D. Newton, *Chem. Rev.*, **91** (1991) 767.
- (2) V. Balzani and F. Scandola, *Supramolecular Photochemistry*; Ellis Horwood: Chichester, England, 1991.
- (3) K. Kalyanasundaram, *Photochemistry of Polypyridine and Porphyrin Complexes*, Academic Press: New York, 1992.
- (4) M. Furue, K. Maruyama, T. Oguni, M. Naiki, and M. Kamachi, *Inorg. Chem.* **31** (1992), 3792.
- (5) M. Furue, T. Yoshidzumi, S. Kinoshita, T. Kushida, S. Nozakura, and M. Kamachi, *Bull. Chem. Soc. Jpn.*, **64** (1991) 1632.
- (6) M. Furue, S. Kinoshita, and T. Kushida, *Chem. Lett.*, (1987) 2355.
- (7) E.M. Kober, J.V. Caspar, R.S. Lumpkin, and T.J. Meyer, *J. Phys. Chem.*, **90** (1986) 3722.
- (8) K.R. Barqawi, Z. Murtaza, and T.J. Meyer, *J. Phys. Chem.*, **95** (1991) 47.
- (9) C.-T. Lin and N. Sutin, *J. Phys. Chem.*, **80** (1976) 97.
- (10) I. Rips and J. Jortner, *J. Chem. Phys.*, **87** (1987) 2090.
- (11) R.A. Marcus and N. Sutin, *Biochim. Biophys. Acta.*, **104** (1985) 265.
- (12) M.J. Weaver, *Chem. Rev.*, **92** (1992) 463.
- (13) G.-H. Lee, L.D. Ciana, and A. Haim, *J. Am. Chem. Soc.*, **111** (1989) 2535.
- (14) K. Nozaki, T. Ohno, and M. Haga, *J. Phys. Chem.*, **96** (1992), 10880.
- (15) J.M. Zaleski, C.K. Chang, G.E. Leroi, R.I. Cukier, and D.G. Nocera, *J. Am. Chem. Soc.*, **114** (1992) 3564.
- (16) Th. Förster, *Discussion Faraday Soc.* **27** (1959) 7.
- (17) D.L. Dexter, *J. Chem. Phys.*, **21** (1953) 836.
- (18) Y.J. Chang, X. Xu, T. Yabe, S.-C. Yu, D.R. Anderson, L.K. Orman, and J.B. Hopkins, *J. Phys. Chem.*, **94** (1990) 729.